VOLUME RENDERING STRATEGIES ON MOBILE DEVICES

José M. Noguera, Juan-Roberto Jiménez, Carlos J. Ogáyar and Rafael J. Segura
Graphics and Geomatic Group of Jaén, University of Jaén, Campus Las Lagunillas, Edificio A3, 23071 Jaén, Spain

Keywords: Volume Rendering, Mobile Devices, GPU, Interactive Frame Rates.

Abstract: This paper proposes and compares several methods for interactive volume rendering in mobile devices. This kind of devices has several restrictions and limitations both in performance and in storage capacity. The paper reviews the suitability of some existing direct volume rendering methods, and proposes a novel approach that takes advantage of the graphics capabilities of modern OpenGL ES 2.0 enabled devices. Several experiments have been carried out to test the behaviour of the described method.

1 INTRODUCTION

Volume visualization is a classic field of computer graphics dedicated to render 3D scalar data. It is essential to engineering and scientific applications that require visualization of three-dimensional data sets.

Until recently, volume visualization has required the use of a desktop computer. There are some cases where this requirement cannot be fulfilled, for instance, teaching labs, operating theatres, field trips, informal meetings, etc. In these cases, it is of use mobile devices, such as mobile phones, tablets or personal digital assistants (PDAs). However, interactive 3D rendering on mobile devices is a challenging task, mainly due to the fact that they must be small and powered by batteries. These two factors severely limit their computing power and memory capacity.

This paper explores how their limited capabilities affect the use of hand-held devices to perform interactive visualization of volumetric data. A novel strategy is proposed, tackling the limitations and special characteristics of mobile devices, that achieves interactive frame rates without recurring to external rendering servers while keeping a good visual quality. This strategy has been implemented and systematically compared with other methods in order to evaluate its performance and visual quality, see Figure 1.

This paper has been structured as follows. Section 2 describes the previous work. Section 3 presents our technique for volume rendering. Section 4 describes the implementation of a volume raycasting technique we have used in our comparison. Section 5 shows and discusses the results under different scenarios. Finally, Section 6 concludes the paper.

(a) (b)

Figure 1: Rendering of a skull model by using a) classic volume ray casting, and b) our texture slicing proposal. Our proposal doubles the performance providing a similar rendering quality.

2 PREVIOUS WORK

A volume can be represented by using different approaches, the usual representation is a set of images/slices that are parallel and evenly distributed across the volume.

In the context of scientific visualization and volume rendering the transport equation usually neglects illumination and is computed by composing colors and opacities of the samples along a given line, for a certain wavelength λ (Levoy, 1988):

M. Noguera J., Jiménez J., J. Ogáyar C. and J. Segura R..
VOLUME RENDERING STRATEGIES ON MOBILE DEVICES.
DOI: 10.5220/0003848604470452
In *Proceedings of the International Conference on Computer Graphics Theory and Applications* (GRAPP-2012), pages 447-452
ISBN: 978-989-8565-02-0

$$C_\lambda(x) = \sum_{k=0}^{n} c_\lambda(x+r_k)\alpha(x+r_k) \prod_{l=k+1}^{n} (1-\alpha(x+r_l)) \tag{1}$$

where $C_\lambda(x)$ is the final color at a given position x, $c_\lambda(x+r_k)$ is the color of the k^{th} sample at position $x+r_k$ inside the volume and $\alpha(x+r_k)$ is its corresponding opacity.

Several methods have been proposed to implement this expression. In general, existing methods can be divided into two categories depending on the way the volume is traversed: object order and image-order approaches. For a deep study about volume rendering techniques we refer to (Weiskopf, 2007).

Ray casting-based volume visualization is a classic image order method (Levoy, 1988) that defines the color of each pixel in the image using the values of a volume taken along a ray originated in that pixel.

Texture-based volume rendering techniques perform the sampling and compositing steps by rendering a set of 2D geometric primitives inside the volume (Ikits et al., 2004). These primitives are usually known as proxy geometry or slices. Each vertex of each primitive has texture coordinates that are used to sample the volume texture. Blending is used to accumulate color values according to corresponding opacities. (Rezk-Salama et al., 2000) presented a technique known as *2D texture slicing*, where the data set is stored as a stack of 2D textures. On the other hand, the *3D texture slicing* technique (Ikits et al., 2004) uses 3D textures and generates a view-aligned group of polygons for each view direction. (Van Gelder and Kim, 1996) avoided this geometry recomputation by using a viewport aligned bounding cube that contains the volumetric model. For each view direction the texture coordinates have to be updated accordingly.

Concerning hand-held devices, interactive direct volume visualization is still a largely unexplored field. In these devices, 3D textures are supported through an optional OpenGL ES 2.0 extension, which is not available in most implementations, e.g., Apple's mobile devices.

First attempts tried to overcome the mobile devices limitations by employing a server-based rendering approach. This approach relies on a dedicated rendering server that carries out the rendering of the volume and streams the resulting images to the mobile client over a network (Lamberti and Sanna, 2005; Jeong and Kaufman, 2007). Also following a server-client scheme, (Zhou et al., 2006) employs a remote server to precompute a compressed iso-surface, which is sent to the mobile device allowing a faster rendering. Unfortunately, these server-based solutions require a persistent and fast network connection.

(Moser and Weiskopf, 2008) introduced an interactive technique for volume rendering on mobile devices that adopts the 2D texture slicing approach. Authors claim to achieve 1.5 frames per second (fps) when rendering a very basic volumetric model consisting of 633 voxels on a Dell Axim x51v device at a resolution of 640×480 pixels.

(ImageVis3D, 2011) is an iOS application that also uses the 2D texture slicing approach. While the user is interacting the number of slices is drastically reduced. At the end of an interaction a new image is rendered with the whole set of slices. This rendering step is carried out in the mobile device itself, or in a remote server in case of complex models.

Recently, (Congote et al., 2011) have implemented a ray-based technique using the WebGL standard. Authors have tested this implementation on some Samsung Galaxy mobile devices, obtaining a frame rate of around 2-3 fps.

3 OUR PROPOSAL

While today's mobile GPUs offer features relatively similar to those found on desktop PCs, their architecture gives preference to energy efficiency rather than to pure performance. Therefore, we cannot expect to run long shaders originally written for desktop PCs on a mobile device at interactive frame rates, even with low screen resolutions (Power VR, 2009). Therefore, shaders for mobile devices must be specifically crafted to avoid complex computations and conditional branches.

The techniques based on 3D texture slicing (Van Gelder and Kim, 1996; Ikits et al., 2004) provide a better rendering quality than the 2D texture slicing approach. However, most OpenGL ES 2.0 implementations available in today's mobile devices do not support 3D textures, so these two techniques do not apply here. Also, the 3D texture slicing technique requires the use of proxy geometry that has to be recomputed every time the viewing angle varies. This representation is not the most appropriate for embedded devices because the best performance on mobile GPUs is obtained by drawing long batches of indexed triangles cached in GPU's memory (Power VR, 2009).

Therefore, our goal is to define a new technique that overcomes these limitations while keeping the same rendering quality.

3.1 Texture Mosaic

In order to provide the mobile GPU with the volumetric data, the set of images that represents the model must be combined into one 2D texture by tiling each

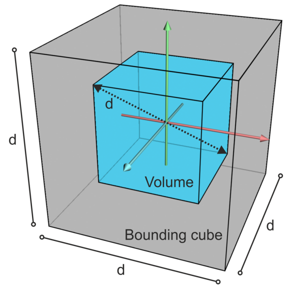

Figure 2: A bounding cube defined around a volume whose diagonal is d.

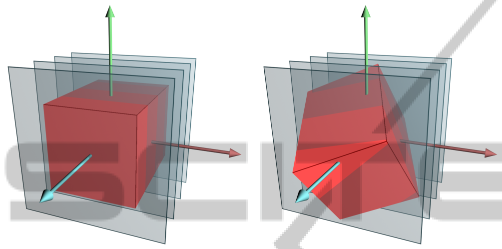

Figure 3: The slices (shown in gray) are always perpendicular to the view direction. The texture coordinates are rotated according to the desired view angle.

image one next to another in a mosaic configuration. This mosaic texture can be generated in a preprocessing step by means of the command-line tool *montage* included in the open-source package *ImageMagick*. In the shader, the correct texture coordinates can be computed as described in (Congote et al., 2011).

3.2 Rendering the Volumetric Model

Our solution consists of a texture slicing approach where a set of slices are projected perpendicular to the view direction. Equation 1 is implemented by compositing these slices in a front-to-back order into the framebuffer using alpha-blending.

Contrarily to the 3D texture slicing approach, in our solution the geometry of the stack of slices is computed once and remains stationary for the rest of the process. Hence, it can be cached in GPU's memory by means of a vertex buffer object (VBO) and reused to draw every frame. VBOs are the preferred method to send geometry to mobile GPUs (Power VR, 2009) because they dramatically reduce the CPU-GPU bandwidth and the number of draw calls.

However, we want to be able to render the model from any angle without the visual artifacts and the waste of memory suffered by the 2D texture slicing approach. In order to render the slices perpendicular to any view direction, the volume is enclosed by a cube of dimensions d^3, being d the diagonal of the volume, see Figure 2. This algorithm is based on Gelder et al. (Van Gelder and Kim, 1996). The front face of the cube remains perpendicular to the view direction and, consequently, the slices defined over it are view-aligned. The 3D texture coordinates without rotation of the vertices of these slices are:

$$(s,t,r) = (\pm\frac{1}{2}\frac{d}{X}, \pm\frac{1}{2}\frac{d}{Y}, \pm\frac{1}{2}\frac{d}{Z}) + (\frac{1}{2}, \frac{1}{2}, \frac{1}{2})$$

where (X,Y,Z) are the dimensions of the texture representing the volume. Then, this texture is properly rotated according to the desired view angle using appropriate transformation of the texture coordinates, see Figure 3.

The proposed implementation works as follows. First, blending should be enabled and configured. The blending factors have been defined in conjunction with code of the shaders to accomplish Equation 1, by using `glBlendFuncSeparate(GL_ONE_MINUS_DST_ALPHA, GL_ONE, GL_ONE, GL_ONE)`.

Then, the GPU is provided with the texture transformation matrix according to the current view and the VBO with the proxy geometry is activated and drawn. The vertex processor receives the vertices, which are transformed according to the model view matrix as usual. The 3D texture coordinates are rotated according to the texture transformation matrix. Listing 1 shows the full GLSL ES (Khronos Group, 2009) code of the corresponding vertex program.

In the fragment shader, the mosaic texture that contains the 3D volume is sampled according to the 3D texture coordinates of the incoming fragment. Then, the value obtained from the volumetric model is used as a texture coordinate for performing a look up in the texture representing the transfer function. Finally, the shader issues the resulting color to be blended in the framebuffer.

Note that those fragments lying outside the volume, that is, those with a texture coordinate component lesser than 0 or greater than 1, have to be discarded. In order to avoid drawing these fragments, (Van Gelder and Kim, 1996) proposed to use six user-defined clip planes around the volume. However, OpenGL ES 2.0 does not support user clip planes by command. At a cost, this behaviour can be emulated in the fragment shader by discarding the referred fragments. Unfortunately, the discard function is very inefficient and its use should be avoided where possible (Power VR, 2011). In our implementation, we avoid it by assigning zero to the alpha component of outside fragments. According to the blending function we use these fragments will not modify the framebuffer.

Listing 2 provides the full GLSL ES code of the fragment program. In this code, the function `getData`

```
attribute vec4 vPos, vTexCoord;
uniform mat4 texCoordRot,prjMat,mvMat;
varying vec4 texCoord;

void main() {
  gl_Position = prjMat*(mvMat*vPos);
  texCoord = texCoordRot*vTexCoord;
}
```

Listing 1: GLSL ES code of the vertex program.

```
uniform float numSlices;
uniform sampler2D modelTex, tfTex;
varying vec4 texCoord;

bool discardOutValues() {
  vec3 zero = vec3(0,0,0);
  if(any(lessThan(texCoord.stp, zero)))
    return true;
  vec3 one = vec3(1,1,1);
  if(any(lessThan(one, texCoord.stp)))
    return true;
  return false;
}

void main (void) {
  if(discardOutValues()){
    gl_FragColor = vec4(0,0,0,0);
  }else{
    float sample = getData(texCoord);
    vec4 color = texture2D(tfTex, vec2(
        sample,0));
    color.a *= (1.0/numSlices);
    color.rgb *= color.a;
    gl_FragColor = color;
  }
}
```

Listing 2: GLSL ES code of the fragment program.

computes the position of the sample inside the mosaic texture, performs the tri-linear interpolation and returns the sample.

4 VOLUME RAY CASTING

In order to test the behaviour of our proposal, we have also implemented a ray casting solution based on (Hadwiger et al., 2009; Congote et al., 2011). A texture mosaic has been used to encode the volumetric model as described in Section 3.1.

The ray is divided into a certain number of steps. A loop in the fragment shader iteratively samples the 3D model applies the transfer function and accumulates the colors and opacities according to Equation 1. The computation stops when the opacity is one or the backside is reached.

5 RESULTS AND DISCUSSION

In our experiments, we selected two popular devices as test platforms, namely, an iPad2 and a 4th generation iPod Touch. The former includes a dual core PowerVR SGX543MP2 GPU whereas the latter features a PowerVR SGX535 GPU. Both devices were running iOS 4.3.5. The software was developed as a native iOS application, written in C++ and GLSL ES.

Two data sets were used in our experiments: the cthuman obtained from the Visible Human Project[1] and the aorta from (Congote et al., 2011). The cthuman model consists of 186 slices of 128×128 pixels each whereas the aorta model has 96 slices of 102×102 pixels. The cthuman and the aorta models were represented by a 2D mosaic of 2048×2048 and 1024×1024 pixels, respectively. Both data sets had 8 bits per sample without texture compression.

Table 1 summarizes the results obtained on the cthuman data set when using the raycasting and our texture-slicing rendering approaches, respectively, and Table 2 the results on the aorta data set. From left to right, the tables show the device used, the screen resolution, and the frame rate obtained while the number of steps or slices increases. The number of steps refers to the number of iterations performed in the raycasting technique (Section 4). On the other hand, the number of slices refers to the number of planes used to sample the model in our technique (Section 3.2). Figure 4 shows the resulting images.

Studying the results summarized in Tables 1 and 2, we observe that, as expected, the performance linearly depends on the number of fragments to be processed and on the number of steps or slices. When using the iPad2 native resolution (1024×768), the number of pixels nearly quadruplicates those used in the iPad2's iPhone compatibility mode (480×320). As a result, the obtained fps also varies in the same proportion.

In our experiments, the iPad2 clearly outperformed the iPod. This stems from the fact that the iPad includes a more powerful GPU. A good rendering quality (40 slices) at a decent frame rate (11 fps) is achieved with this device. This result proves that it is possible to render volumetric models on mobile devices while an interactive frame rate is guaranteed.

When comparing both techniques, we have to keep in mind the differences between them. The volume ray casting approach computes the accumulation along a given ray by iterating inside the shader. On the contrary, our approach substitutes this iteration by processing in parallel simpler fragments for each one of the slices. According to our experiments, see

[1] http://www.nlm.nih.gov/research/visible/visible_human.html

Table 1: Timing for rendering the cthuman model with different devices, image resolutions and number of steps or slices.

		Ray Casting					Our approach			
Device	Resolution	10	20	40	80		10	20	40	80
iPad2	480 × 320	23.5 fps	12.1 fps	6.4 fps	3.4 fps		40.1 fps	21.7 fps	11 fps	5.5 fps
iPad2	1024 × 768	5.2 fps	2.8 fps	1.4 fps	1.4 fps		10.3 fps	5 fps	2.4 fps	1.3 fps
iPod	480 × 320	3.2 fps	1.9 fps	1.6 fps	1 fps		6.6 fps	3.2 fps	1.5 fps	1.4 fps

Table 2: Timing for rendering the aorta model with different devices, image resolutions and number of steps or slices.

		Ray Casting					Our approach			
Device	Resolution	10	20	40	80		10	20	40	80
iPad2	480 × 320	23.2 fps	12.3 fps	6.5 fps	3.2 fps		45.4 fps	22.2 fps	11 fps	5.4 fps
iPad2	1024 × 768	5.1 fps	2.8 fps	1.5 fps	1.4 fps		10.3 fps	4.8 fps	2.4 fps	1.2 fps
iPod	480 × 320	3.1 fps	1.7 fps	1.6 fps	1.2 fps		6.6 fps	3.2 fps	1.5 fps	1.5 fps

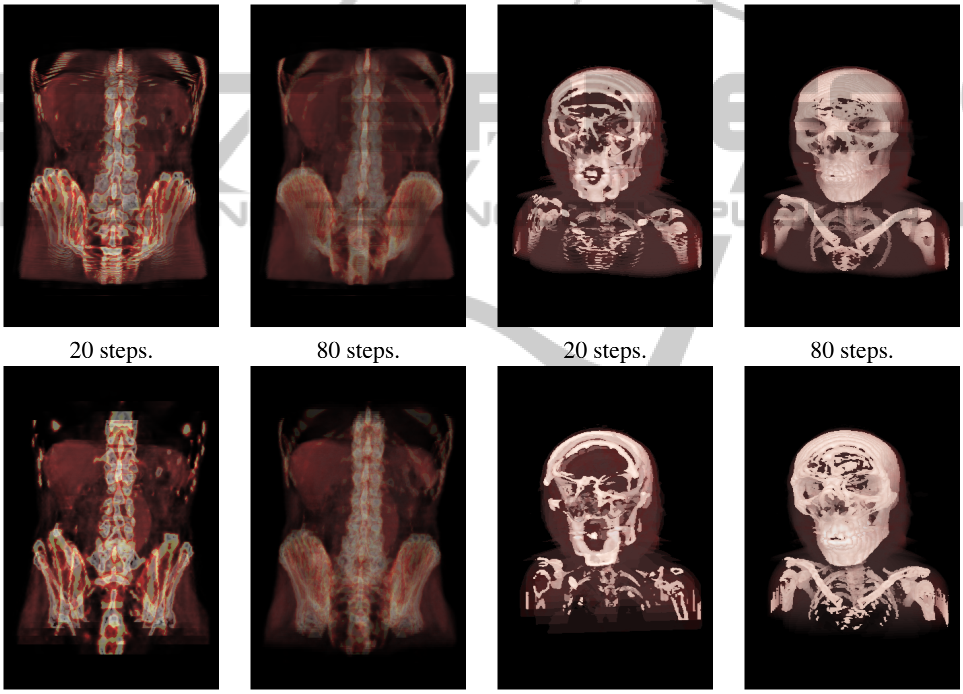

20 steps. 80 steps. 20 steps. 80 steps.

20 slices. 80 slices. 20 slices. 80 slices.

Figure 4: Images from the aorta and cthead models with different number of steps/slices. Top: raycasting approach. Bottom: our texture slicing approach.

Tables 1 and 2, our texture-slicing approach nearly doubles the performance obtained by the ray casting technique. These results suggest that it is preferable to compute a larger amount of short fragments rather than a few of them with a more complex behaviour.

We believe that, as the number of processing cores in mobile GPUs increases, the performance gain of our technique when compared to the ray-based solution will also increase, allowing a truly interactive solution to become a reality in this kind of devices.

However, the ray-based technique provides a better rendering quality. Figure 4 compares both approaches for an increasing number of steps/slices. We notice that the number of slices must be greater than the number of steps to achieve similar results, due to the fact that the slices are defined over the bounding box and some of them can be out of the model.

We have also observed that mobile GPUs are, in general, less intuitive and more unpredictable in their performance that their desktop counterparts. It is paramount to avoid branching in shader programs for a mobile GPU. Although theoretically branching is fully supported, including one single if-else clause can slow down the performance up to 20 fps.

Finally, we want to point out another consideration related to the mobile GPU architectures used in our experiments. PowerVR graphics processors heavily rely on a method called Tile Based Deferred Rendering (TBDR) (Power VR, 2011) to achieve good rendering performance while keeping low energy consumption. TBDR allows to perform hidden surface removal before fragments are processed thus avoiding unnecessarily computations. Unfortunately, this hardware optimization is not well suited for volume rendering. The texture slicing technique requires blending, which forces to process all fragments. In our experiments, turning off blending boosted the performance to 60 fps regardless of the number of slices rendered. The raycasting technique does not benefit from this technique because there is no fragments overlap so no computation can be avoided.

6 CONCLUSIONS

We have developed a novel volume rendering algorithm perfectly suited to modern GPU-enabled mobile devices. This proposal has addressed the limitations of these devices, mainly the lack of 3D texture support and the limited complexity that can be imbued to shaders. Our method has been tested under different devices and scenarios. We have also compared our results with the volume ray casting method. In general, our experiments show that the ray-based method provides a slightly higher quality image, whereas our texture slicing method doubles the frame rate.

Our work has shown that mobile devices constitutes a valid platform to achieve interactive volume visualization, despite the fact that the rendering capabilities are reduced in comparison to desktop solutions, due to their inherent autonomy limitations.

As future work, our current research is focused on the improvement of the rendering performance and quality based on a continuous search of new techniques well suited to this kind of devices. We also plan to improve the visual appearance by including complex illumination in our models.

In addition, we plan to use our experience and this technology in university teaching, for instance in subjects like human anatomy, diagnosis, etc. We believe that interactive visualization of medical data in handheld devices can be a worthy pedagogic instrument.

ACKNOWLEDGEMENTS

This work has been partially supported by the Ministerio de Ciencia e Innovación and the European Union (via ERDF funds) through the research project TIN2011-25259 and by the University of Jaén through the projects PID441012 and UJA2010/13/08 sponsored by Caja Rural de Jaén.

REFERENCES

Congote, J., Segura, A., Kabongo, L., Moreno, A., Posada, J., and Ruiz, O. (2011). Interactive visualization of volumetric data with webgl in real-time. In *Proceedings of the Web3D '11*, pages 137–146. ACM.

Hadwiger, M., Ljung, P., Salama, C. R., and Ropinski, T. (2009). Advanced illumination techniques for gpu-based volume raycasting. In *ACM SIGGRAPH 2009 Courses*, pages 2:1–2:166. ACM.

Ikits, M., Kniss, J., Lefohn, A., and Hansen, C. (2004). *GPU Gems II*, chapter Volume Rendering Techniques, pages 667 – 692. Addison Wesley.

ImageVis3D (2011). Imagevis3d: A real-time volume rendering tool for large data. scientific computing and imaging institute (sci).

Jeong, S. and Kaufman, A. E. (2007). Interactive wireless virtual colonoscopy. *The Visual Computer*, 23(8):545–557.

Khronos Group (2009). *The OpenGL ES Shading Language*, 1.00 edition.

Lamberti, F. and Sanna, A. (2005). A solution for displaying medical data models on mobile devices. In *SEPADS'05*, pages 1–7, Stevens Point, Wisconsin, USA. (WSEAS).

Levoy, M. (1988). Display of surfaces from volume data. *Computer Graphics and Applications, IEEE*, 8(3):29 –37.

Moser, M. and Weiskopf, D. (2008). Interactive Volume Rendering on Mobile Devices. In *Workshop on Vision, Modelling, and Visualization VMV '08*, pages 217–226.

Power VR (2009). PowerVR SGX OpenGL ES 2.0 application development recommendations.

Power VR (2011). PowerVR Series5 Graphics SGX architecture guide for developers.

Rezk-Salama, C., Engel, K., Bauer, M., Greiner, G., and Ertl, T. (2000). Interactive volume on standard pc graphics hardware using multi-textures and multi-stage rasterization. In *Proceedings of the ACM SIGGRAPH/EUROGRAPHICS workshop on Graphics hardware*, HWWS '00, pages 109–118. ACM.

Van Gelder, A. and Kim, K. (1996). Direct volume rendering with shading via three-dimensional textures. In *Proceedings of the 1996 symposium on Volume visualization*, VVS '96, pages 23–ff., Piscataway, NJ, USA. IEEE Press.

Weiskopf, D. (2007). *GPU-based interactive visualization techniques*. Mathematics and visualization. Springer.

Zhou, H., Qu, H., Wu, Y., and yuen Chan, M. (2006). Volume visualization on mobile devices. In *14th Pacific Conference on Computer Graphics and Applications*, pages 76–84.